

CONSTRUCTION OF DECISION REGION BORDERS BY GEOMETRIC MODELLING OF TRAINING SETS

Application to land cover classes in remotely sensed images.

T. BARATA, P. PINA

CVRM / Centro de Geo-Sistemas, Instituto Superior Técnico

Av. Rovisco Pais, 1049-001 Lisboa, PORTUGAL

Abstract In this paper a novel methodology to construct decision region borders that geometrically models the training sets of points is presented. It is shown that with the incorporation of the features of the training sets more correct decision borders are designed and, in consequence, higher classification rates are obtained. This methodology is completely based on mathematical morphology operators and is illustrated with two features (wetness' tasselled cap and *NDVI*'s vegetation index) of seven land cover classes (forest (3), soil (2), vegetation and water) constructed from remotely sensed images of a region in centre Portugal.

Keywords: elementary textural units, decision borders regions, directional structuring elements, anisotropic distance function, classification.

1. Introduction

Although the geometric modelling of training sets performed by the majority of classification approaches is rather poor when complex and irregular shapes appear, the effort put on modelling its geometry in features space has been small and, consequently, the achieved results not always very satisfying. Naturally, the most interesting and promising approaches in dealing with this type of geometric modelling have been proposed in the frame of mathematical morphology. One of the first attempts was made by Madier *et al.* [8] in the classification of remotely sensed images. More recently studies, by Soille [14, 15] in the segmentation by watershed of features space to land use unsupervised classification, by Muge *et al.* [10] in a geochemical exploration application to create maps of favorability of occurrence of mineral resources, by Park *et al.* [11] for colour images segmentation, or by Breen [5] introducing the closing function notion to segment non-image data, have shown the potentialities of using mathematical

morphology to model the geometry of complex and irregular training sets of points.

In this paper, it is intended to explore the features presented by the training sets of each class (size, shape and orientation) in order to construct the respective decision regions borders without making explicitly any statistical hypothesis. Previously, the elementary units of the images to be classified are defined, not according to the digital picture elements (pixels), but according to its texture.

2. Data available and selection of features

The data used to develop this methodology consists on Landsat 5 TM satellite images (6 bands with a spatial resolution of 30 metres/pixel, each one with 256 gray levels) from October 1997 of a rural region in centre Portugal of about 39 x 36 km² (images of 1289 x 1205 pixels). Additional information, as aerial photographs with geometric corrections performed (true colour orthophotomaps with a spatial resolution of 1 metre/pixel) were also available and were used to help identify the different land cover classes in the construction of ground truth images. Seven different land cover classes are constituted: three forest cover types (olive, cork oak and pine+eucalyptus trees), two types of soil (bared and mixed), one type of vegetation and also water.

The methodology presented in this paper, although conceived to be applied in a n -dimensional feature space is, presently, only performed on a two-dimensional feature space. An exploratory analysis of the original images shows a very similar behavior for the different land cover classes sampled in a semi-automatic approach [1], denoting a very high overlapping for every projected pair of possible combinations [2]. The construction of indirect variables, a common procedure in remote sensing applications in order to enhance the separability between the different cover classes, was then tested. After several experiments, the pair of variables that has shown a higher separability between classes consisted of a wetness variable and a vegetation index.

The wetness variable (W) is obtained through the tasseled cap transform, originally proposed by Kauth and Thomas [7] and informs about the content of water or humidity in the earth's surface. In the corresponding image for the region under study presented in figure 1a) the lighter values indicate a higher value of humidity while darker values denote lower humidity in Earth's surface.

The other variable consists on the normalized difference vegetation index ($NDVI$) [9] and corresponds to the degree of vegetated covers (forest, vegetation) in the images. The absence or low contribution of vegetated covers results in darker regions of this index image, while the opposite situation results in lighter regions (see the obtained image in figure 1b).

Other indirect features tested and combined have consisted on the other two tasseled cap axes (brightness and greenness), other vegetation axis (GVI, SAVI, STVI3) and Principal Component Analysis axes.

3. Definition of elementary textural units

Due to the richness and complexity of remotely sensed images it is preferable to use an object-based classification instead of a pixel-based approach. Its elementary textural units can be, for instance, the catchment basins of the image, when thinking on the application of the watershed transform. In order to segment all similar regions the watershed transform is then used and it is based on the gradient version using its minima as markers [3, 4]. Since, at least two variables are used, a multi-spectral version of this transform must be used. The multi-spectral gradient, $mgrad$, computed on the W and $NDVI$ variables appeals to Soille's definition [14, 15], being its minima the markers used to compute the multi-spectral watershed whose simplified approach ($Wsh(W, NDVI)$) is resumed by the following expression:

$$Wsh(W, NDVI) = [[Sk_L[Wsh_{mgrad}(W) \cup Wsh_{mgrad}(NDVI)]] \circ E]_\infty \quad (1)$$

The union of individual watersheds ($Wsh(W)$ and $Wsh(NDVI)$), besides creating more basins, may also create watershed lines with a thickness superior to one pixel. To reduce this set to one pixel thickness, the skeleton obtained with the letter L of Golay alphabet [12], Sk_L , followed by a pruning till idempotence (neighborhood transform, \circ , with letter E of Golay alphabet [12]) is performed. Each catchment basin corresponds now to one elementary textural unit of the landscape to be classified, divided by one pixel thick crest lines.

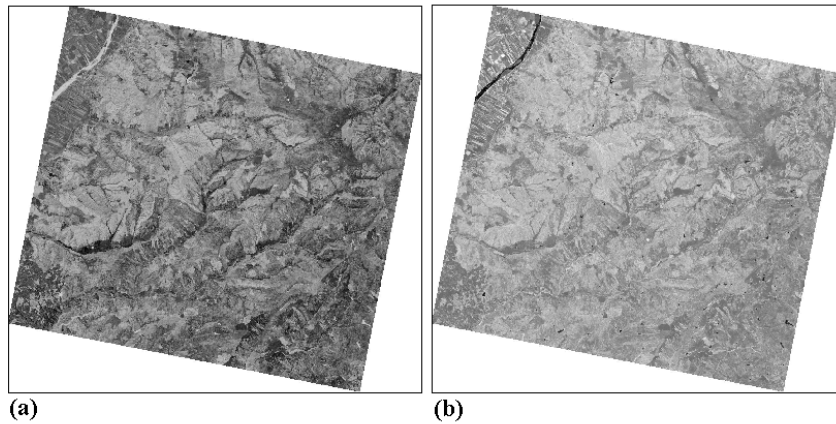


Figure 1. Images of a region in centre Portugal corresponding to the features used: (a) wetness (W) and (b) $NDVI$.

4. Creation of strong nucleus for each class

A morphological based clustering to create strong nuclei, *i.e.*, more compact nuclei, is achieved through sequences based on alternating (AF) or alternat-

ing sequential filters (ASF) [13]. The sequence should start with a closing transform φ in order to connect the original plotted points X , that normally present a certain spatial dispersion degree. The application of the opening γ in the sequence has the effect of filtering the weaker (smaller and more distant) clusters of points. Since, each class k is processed individually, it is necessary to identify and to remove all overlapping regions between the different nuclei obtained. The following expression resumes, for an AF sequence $\gamma_i\varphi_i$, these operations. The resulting set Y , union of all n nuclei k is obtained as follows:

$$Y = \bigcup_{k=1,n} [\gamma_i\varphi_i(X_k)] / \bigcap_{k=1,n} [\gamma_i\varphi_i(X_k)] \quad (2)$$

Several experiments were made, in an empirical way, by testing different dimensions of the structuring elements (hexagons) over the sets of projected points of each class, whose coordinates represent the average values of the pixels within each catchment basin for W (y -axis) and $NDVI$ (x -axis) features (figure 2a). An example showing the application of an alternating filter of opening-closing type of size 5 to the projected points of figure 2a is shown in figure 2b. Each class is now represented by compact nucleus that, depending on the type of clustering performed, may be constituted by one or more connected components.

5. Determination of decision regions borders

The strong nucleus of each class are now the basis for the determination of the corresponding decision regions borders. To design these borders two situations are envisaged, one that admits that the influence zone of each nucleus is based on an Euclidean distance and another one that admits that it should depend on the features (size, shape and orientation) of each nucleus.

5.1 BASED ON ISOTROPIC INFLUENCE ZONES (MM1)

In this situation the determination of the decision regions for each class can be simply obtained through a skeleton by influence zones transform (*SKIZ*). The space partition obtained is presented in figure 2c, being the border points of the binary image assigned to the most frequent class in its neighborhood by a novel morphological algorithm [2]. The development of this algorithm results from the necessity of not taking into account the watershed points that lie in the neighborhood of each analysed pixel when the most frequent class is computed. Moreover, this algorithm by using directional dilations and set intersections between each class and the watershed lines is computed simultaneously for all the pixels of the image.

This may result in the modification of the connexity number, through the merging of adjacent regions that belong to the same class like, for instance, the three cork oak nuclei in figure 2b that are merged into a single region in figure 2c.

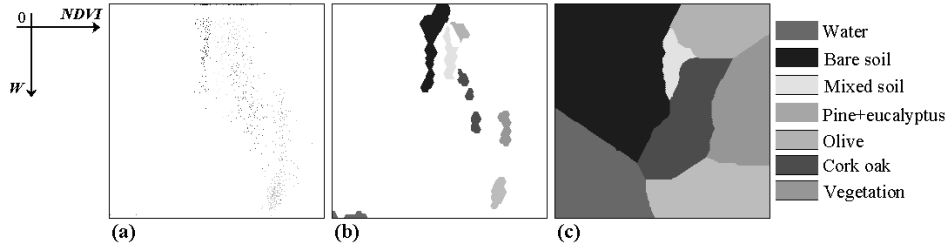


Figure 2. (a) Projection of textural elements in W - $NDVI$ space, (b) Nuclei obtained by application of an AF of size 5 and (c) Decision regions obtained by the SKIZ of the nuclei.

5.2 BASED ON WEIGHTED INFLUENCE ZONES (MM2)

Finding the best decision region borders should not simply depend on an isotropic influence zone, but also on the geometric features of the nuclei obtained. By analysing the nuclei obtained (figure 2b) it is clearly noticeable that the size, shape, orientation and also the connexity number are characteristic of each class. In order to construct each decision region according to these features, an algorithm to design these borders in 4 main steps is proposed in the following.

Computation of preferential alignments. Several procedures to compute preferential alignments of structures can be found in the literature, being the roses of directions and intercepts [6] the most common ones in the mathematical morphology universe. The computation of the rose of directions based on neighborhood transforms [12] is the one adopted here. The values obtained for the nuclei of figure 2b are presented in table 1 and respect only relative values for 3 main directions (0° - 60° - 120° or 30° - 90° - 150°) according to the minimum obtained for each direction. The rose of directions of classes constituted by more than one connected component (like cork oak class) are computed with the contribution of individual cluster values.

Table 1. Relative preferential alignments of the nuclei (using 3 directions in the hexagonal grid).

0°	30°	60°	90°	120°	150°
10	-	1	-	1	-
-	2	-	8	-	1
-	1	-	3	-	1
1	-	15	-	2	-
-	1	-	6	-	15
1	-	1	-	3	-
-	1	-	15	-	1

Construction of structuring elements. The construction of structuring elements based on the shape and size of the similar features of the respective nuclei, is identical to the construction of nD structuring elements from a $(n-1)D$ space. For instance in a $2D$ space, the corresponding structuring elements are constructed using line segments criteriously oriented, *i.e.*, are constructed from successive directional dilations in the main directions of the digital grid used [12]. For the nuclei of figure 2b, using the values of the corresponding rose of directions (table 1), the structuring elements constructed with sequences of directional dilations are shown in figure 3. Besides the different dimensions, it is clearly noticeable that all structuring elements are anisotropic.

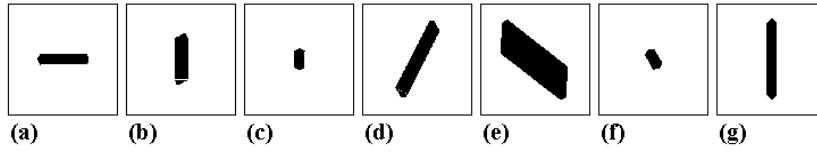


Figure 3. Structuring elements (with dimensions presented in table 1) resuming nuclei features for class: (a) water, (b) bare soil, (c) mixed soil, (d) pine and eucalyptus, (e) olive, (f) cork oak, (g) vegetation.

Distance function construction. The influence zone of each class is then computed according to the orientation and size of each nucleus. In practice, it is quite difficult to compute all these influence zones simultaneously, *i.e.*, to make each nucleus grow with different velocity and orientation. Alternatively, one proposes to first compute the distance function $d_f(Y_k)$ for each nucleus k using its own structuring element. The pixels closer to the nucleus have a lower distance value to the nucleus while the pixels farther have a higher distance value. The gray level in the corresponding image is directly proportional to the distance: lighter gray levels correspond to higher distances while darker gray levels correspond to lower distances. In figure 4 the different distance functions obtained for each class k for the complete feature space are presented. Each distance function exhibits now the same features presented by its nucleus.

Decision region borders computation. The design of the decision regions borders for each class is based on the computation of the influence zone of the nucleus of each class through the different distance functions obtained. The computation of the inf of the seven distance functions used gives a global distance function, $d_f(Y)$ that correspond to the influence zone of each nucleus:

$$d_f(Y) = \inf[d_f(Y_k)] \quad (3)$$

In this image, each influence zone corresponds to a catchment basin. Thus, the computation of the watershed transform produces the decision region borders $drb(Y_k)$ of each class or nucleus k :

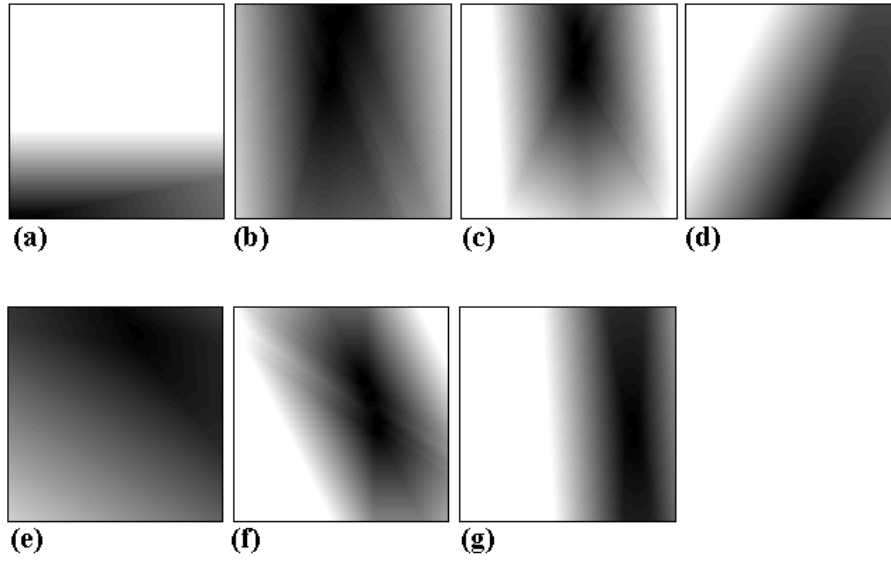


Figure 4. Distance functions for class: (a) water, (b) bare soil, (c) mixed soil, (d) pine and eucalyptus, (e) olive, (f) cork oak, (g) vegetation.

$$drb(Y_k) = Wsh[d_f(Y)] \tag{4}$$

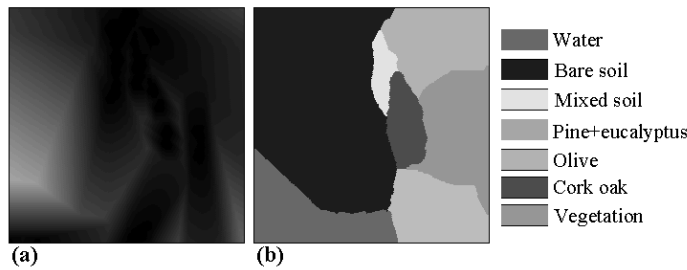


Figure 5. (a) Global distance function (inf of individual distance functions) and (b) Decision regions borders.

The partition obtained (figure 5b) presents now a quite different aspect, where the orientations of the original clusters of each class are now noticeable, which was not the case in the previous partition (figure 2c).

6. Land cover classification

Using the partition obtained each elementary textural element can be classified accordingly. An example of the classified image for the region under study in presented in figure 6. In table 2 the classification rates obtained for each land

Table 2. Classification rates (omission errors (%)).

<i>classes</i>	MD	ML	MM1	MM2
water	1.63	1.69	1.63	1.69
bare soil	31.34	26.78	32.93	9.86
mixed soil	99.94	97.32	69.97	52.24
pine+eucalyptus	0.48	15.13	17.85	14.21
cork oak	46.70	90.79	55.04	66.27
olive	98.87	52.13	5.42	9.28
vegetation	100.00	55.66	48.03	47.23
<i>KIA</i>	0.4489	0.5448	0.6640	0.7651

use class are also presented and refer to two test regions (dimension of 463 x 382 and 150 x 205 pixels) chosen from the larger region under study (1289 x 1205 pixels). These rates (MM2) concern the omission errors (number of pixels in the ground truth image that were mis-classified) and are compared not only with the results obtained by using the partition obtained with isotropic structuring elements (MM1) but also by the application of two of the most popular methods in remote sensing: minimum distance (MD) and maximum likelihood (ML). The same set of input data features is used by these 4 classification approaches and an overall accuracy, given by the *Kappa Index Agreement (KIA)* [9], is used to compare the global results obtained by each method (values obtained are also presented in table 2).

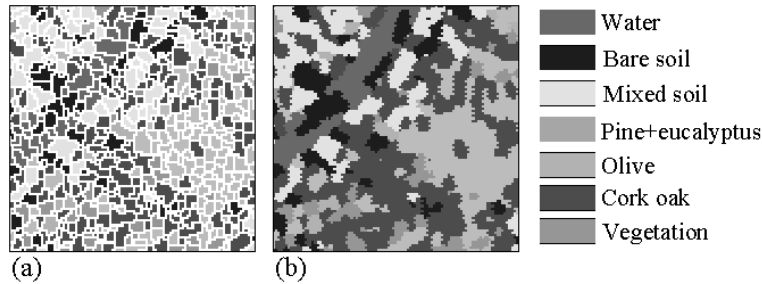


Figure 6. Classified image (detail) using the MM2 approach: (a) with watershed lines (in white) and (b) without watershed lines (assigned to the most frequent class in the neighborhood of each point).

Analysing the classification rates, it can be concluded that the global improvement provided by the proposed methodology is quite impressive. In general, the overall results provided by the novel approaches (MM1 and MM2) are better (*KIA* values of 0.6640 and 0.7651, respectively) than the ones obtained through common approaches (MD and ML with *KIA* equal to 0.4489 and 0.5448). Although MD method classifies almost correctly 2 classes (water and pine+eucalyptus trees with errors near 0%) it misses completely 3 other

classes (mixed soil, olive trees and vegetation with errors close to 100%). The ML method, which normally performs a slightly better geometric modelling, is not so severe and, although mixed soil and cork oak classes present errors above 90%, gives better results than MD method. The MM1 approach presents higher rates than these classic approaches, which is a direct reflex of a more correct geometric modelling of the training sets. The incorporation of the geometric features of the training sets into the creation of the partition (MM2) improves even more these rates.

7. Conclusions and future developments

This paper reinforces that the geometric modelling of the training sets is an important improvement in the classification procedures, as the higher classification rates obtained, in comparison to the ones obtained with traditional approaches, demonstrate.

The main future developments intended to pursue in order to improve and consolidate this methodology, include its extension to a n -dimensional features space, the possibility of locally displacing the decision region borders and the definition of objective criteria for the automatic construction of the nucleus of each class.

References

- [1] T. Barata, P. Pina, I. Granado. Segmenting at higher scales to classify at lower scales. A mathematical morphology based approach applied to forest cover remote sensing images. In A. Sanfeliu, J.J. Villanueva, M. Vanrell, R. Alquézar, J. Crowley and Y. Shirai, editors, *Proceedings of ICPR'2000 - 15th International Conference on Pattern Recognition-Barcelona, Spain*, vol.4, pages 84–87, Los Alamitos, 2000. IEEE Computer Society.
- [2] T. Barata. Classification of forest covers in remotely sensed images through a mathematical morphology based methodology (in portuguese). PhD thesis, Technical University of Lisboa, Lisboa, 2001.
- [3] S. Beucher. Segmentation d'images et morphologie mathématique. Thèse de doctorat, ENSMP, Paris, 1990.
- [4] S. Beucher, F. Meyer. The morphological approach to segmentation: The watershed transformation. In E. Dougherty, editor, *Mathematical Morphology in Image Processing*, pages 433–482, New York, 1993. Marcel Dekker.
- [5] E. Breen. Morphological segmentation of non-image data. The closing function. In H. Heijmans and J. Roerdink, editors, *Mathematical Morphology and its Applications to Signal and Image Processing*, pages 223–230, Dordrecht, 1998. Kluwer Academic Publishers.
- [6] J.L. Chermant, M. Coster. *Précis d'analyse d'images*. 2ème edition. Presses du CNRS, Paris, 1989.
- [7] R.J. Kauth, G. Thomas. The tasseled cap - a graphic description of the spectral-temporal development of agricultural crops as seen by Landsat. In *Proceedings of the Symposium on Machine Processing of Remotely-Sensed Data*, vol. 4B, pages 41–51, Purdue University, West Lafayette, 1976.

- [8] J.P. Madier, G. Flouzat, M. Jourlin. A non-parametric supervised multispectral classification method using binary morphological operators. In *Proceedings of IGARSS'86 Symposium*, ESA-SP-254, vol. 1, pages 547–552, Zurich, 1986.
- [9] P. Mather. *Computer processing of remotely-sensed images. An introduction*. 2nd edition, J. Wiley and Sons, New York, 1999.
- [10] F. Muge, P. Pina. Applications of morphological operators to supervised multidimensional data classification. In J. Serra and P. Soille, editors, *Mathematical Morphology and its Applications to Signal and Image Processing*, pages 361–368, Dordrecht, 1994. Kluwer Academic Publishers.
- [11] S.H. Park, I.D. Yun, S.U. Lee. Color image segmentation based on 3-D clustering: Morphological approach. *Pattern Recognition*, 31(8):1061–1076, 1998.
- [12] J. Serra. *Image analysis and mathematical morphology*. Academic Press, London, 1982.
- [13] J. Serra (editor). *Image analysis and mathematical morphology, vol.2: Theoretical advances*. Academic Press, London, 1988.
- [14] P. Soille. Morphologie Mathématique: Du relief à la dimensionalité. Algorithmes et méthodes. Thèse de doctorat, Université Catholique de Louvain, Louvain, 1992.
- [15] P. Soille. *Morphological image analysis. Principles and applications*. Springer, Berlin, 1999.